JOURNAL OF APPLIED ELECTROCHEMISTRY **29** (1999) 123–128

Inhibiting effect of citric acid on the pitting corrosion of tin

C. M. V. B. ALMEIDA, T. RABÓCZKAY

Instituto de Química da Universidade de São Paulo, PO Box 26077, 05599-970, São Paulo, SP, Brazil

B. F. GIANNETTI

**Instituto de Ciências Exatas e Tecnologia da Universidade Paulista, R. Dr. Bacelar 1212, 04026-002, São Paulo, SP, Brazil*

Received 9 April 1997; accepted in revised form 21 April 1998

Potentiostatic and potentiodynamic studies were carried out to establish the inhibiting effects of citric acid on the pitting corrosion of tin. The critical potential (E_{crit}), which leads to pitting or general corrosion, was determined in sodium perchlorate solution in the pH range 1.0 to 4.0. Pit nucleation and growth, at pH 4.0, can be described by instantaneous nucleation followed by progressive nucleation. The results show that the minimum acid concentration needed to inhibit pitting of tin is 10^{-2} M. Pitting occurrence by direct interaction between metal and perchlorate anions was observed.

Keywords: *tin*, *perchlorate*, *citric acid*, *pitting*, *inhibition*

1. Introduction

The electrochemical behaviour of tin is of interest due to its widespread technological application. A relatively large amount of work has focussed on the electrochemical behaviour of the metal in the presence of organic acids [1–20]. These acids are naturally present in canned food and, therefore, they participate directly in the electrochemical corrosion and/or passivation of the metal.

General corrosion of tin is observed in pure citric acid revealing a surface that shows anisotropic reflection of polarized light. Several authors report that pitting corrosion occurs when the surface is exposed to aqueous solutions containing aggressive anions such as halides [21]. However, this form of localized corrosion may also occur in the presence of other species such as perchlorate, sulphate and nitrate anions [22–25].

The dissimilar character of the corrosion observed for citric and perchlorate media stimulated interest in the study of the electrochemical behaviour of tin in solutions containing the two anions (perchlorate and citrate), with special emphasis on the determination of which interaction anion/surface prevails and on the influence of citric acid concentration on the nature of the corrosion. The present paper relates the influence of the potential, pH and citric acid concentration on the corrosion of tin in 0.5 M $NaClO_4$. The possibility of the citrate anion improving resistance to pitting corrosion was also investigated.

2. Experimental details

Potentiodynamic and potentiostatic measurements were carried out in a standard electrochemical cell. A tin disc with an exposed geometric area of 0.64 cm^2 mounted in polyester resin was used as working electrode. The reference electrode was a reversible hydrogen electrode placed in a Luggin–Haber capillary and the counter electrode was a platinized platinum wire of large area. The electrolytes, 0.5 M $NaClO_4$ and 10^{-9} to 10^{-1} M citric acid, were prepared from Merck p.a. grade reagents and triply distilled water. Solutions of pH 1.0, 2.0, 3.0 and 4.0 were obtained by addition of perchloric acid. Before each experiment, the surface of the electrode was wet-ground with abrasive grade 600 mesh paper, washed quickly with triply distilled water and immersed in the electrolytic solution. Nitrogen was bubbled through the cell to deaerate the solution. To avoid perchlorate reduction at tin electrodes, the initial potential of the experiments was fixed at −0.5 V [22]. A metallographic microscope coupled to a Polaroid ™ camera was used to observe the electrode surface. Potentials quoted in this text are given on the standard hydrogen scale. All experiments were carried out at 25 °C.

3. Results and discussion

3.1. *Tin/perchlorate system*

The critical potential (E_{crit}) of tin in 0.5 M sodium perchlorate was determined to characterise the metal

resistance to corrosion in this solution. As the type of corrosion was found to be pH dependent, the term critical potential, for either pitting or general corrosion, was used in order to simplify terminology. Two electrochemical methods were employed to determine E_{crit}: potentiostatic (Fig. 1) and potentiodynamic with a scan rate of $0.5\,mV\,s^{-1}$ (Fig. 2).

Before the additions of citric acid to the system, the potentiostatic current transients obtained at pH 3.0 and 4.0 were analysed. Current transients associated with pit growth involve several contributions which may be evaluated by an appropriate selection of the applied potential (E). Thus, potentiostatic current transients were run for both $E < E_{crit}$ and $E \geqslant E_{crit}$.

3.1.1. Current transients recorded when $E < E_{crit}$. When the applied potential is more negative than the critical potential, the overall anodic current density, j, can be considered as the sum of two terms:

$$j = j_{dl} + j_{ox} \quad (1)$$

where j_{ox} is related to the oxide formation. The double layer charging component, j_{dl}, drops to zero in time; therefore, in the time domain of this study, its contribution can be neglected.

During metal oxidation intense dissolution of tin occurs [28–31]. On the other hand, the formation of an oxide film is indicated by the presence of a current peak at about −0.35 V (Fig. 2). Thus, the oxide formation mechanism may be described as a result of metal dissolution followed by hydroxide formation [32] and the main steps of the anodic process may be assigned to the following reactions:

$$Sn \underset{k_b}{\overset{k_f}{\rightleftharpoons}} Sn^{2+} + 2\,e^- \quad (2)$$

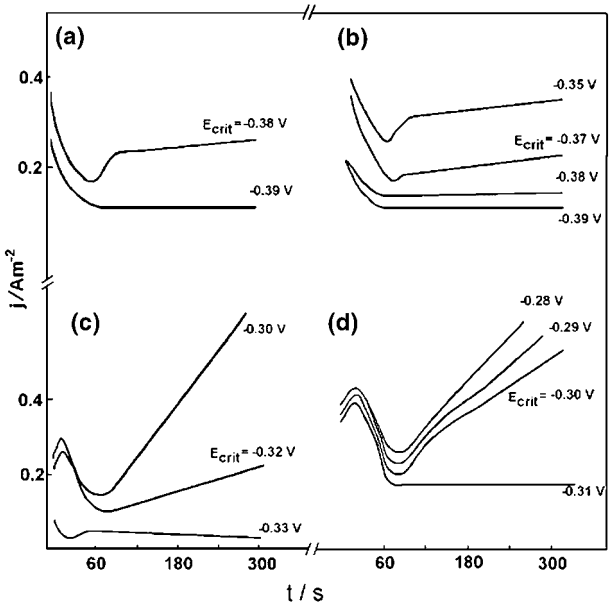

Fig. 1. Current density as a function of time at constant potential in 0.5 M $NaClO_4$: (a) pH 1.0, $E_{crit} = -0.38$ V; (b) pH 2.0, $E_{crit} = -0.37$ V; (c) pH 3.0, $E_{crit} = -0.32$ V and (d) pH 4.0, $E_{crit} = -0.30$ V.

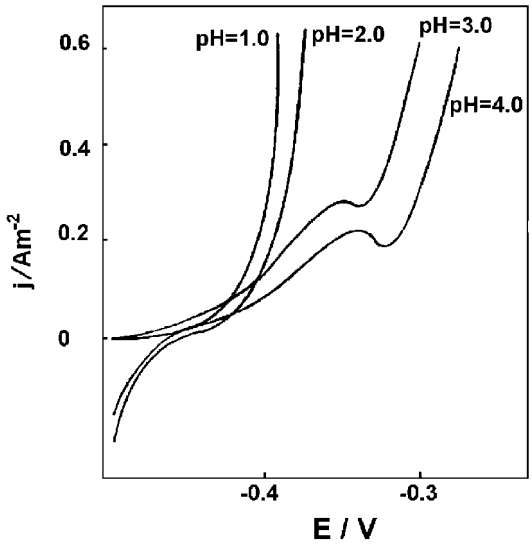

Fig. 2. Polarization curves of tin in $NaClO_4$ 0.5 M, $v = 0.5\,mV\,s^{-1}$, at pH 1.0, 2.0, 3.0 and 4.0.

$$Sn^{2+} + 4\,H_2O \rightleftharpoons Sn(OH)_4 + 4\,H^+ + 2\,e^- \quad (3)$$

According to Ogura's model [32], the current related to the oxide formation, j_{ox}, is given by

$$j_{ox} = \frac{P_1}{(t+P_2)^{1/2}} + P_1 P_2^{1/2} \mathrm{erf}(P_2 t)^{1/2} \quad (4)$$

where the constant parameters of Equation 4 are

$$P_1 = nFD_o^{1/2}(1 + 1/K)C_o^{sat}\pi^{-1/2} \quad (5)$$

$$P_2 = k_f + k_b \quad (6)$$

and where D_o is the metallic hydroxide diffusion coefficient, k_f and k_b are the forward and backward rate constants of Reaction 2, respectively, C_o^{sat} is the saturation concentration of the metallic hydroxide at the electrode surface, K is the equilibrium constant of Reaction 2 and n and F have their usual meaning.

The P_1 and P_2 values resulting from the fitting of the experimental data to Equation 4 are shown on Table 1. Comparison of the potentiostatic current transient obtained with Equation 4 and the experimental data (Fig. 3) allows use of Ogura's model [32] to describe j_{ox}.

3.1.2. Current transients recorded when $E \geqslant E_{crit}$. Figure 1(d) shows that, after oxide formation and $t \geqslant 60$ s, a considerable current increase occurs. Therefore, a new term, j_p, related to the pit growth current, must be included to represent the total cur-

Table 1. Parameters resulting from the fitting of experimental data to Equation 4

E/V	pH	$10^4 \times P_1$/A $s^{1/2}$ m^{-2}	P_2/s^{-1}
−0.33	3	1.8 ± 0.3	10.1 ± 0.3
−0.31	4	25.1 ± 2.7	2.9 ± 0.3

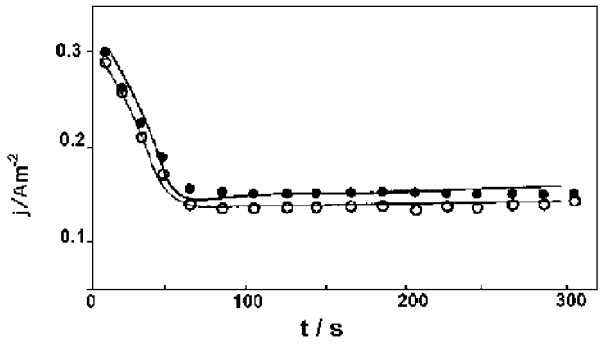

Fig. 3. Current transients obtained at $E < E_{crit}$, in 0.5 M $NaClO_4$. Symbols denote experimental data: (●) $E = -0.31$ V, pH 4.0; (○) $E = -0.33$ V, pH 3.0 and solid lines correspond to current transients calculated with Equation 4.

rent density. Thus, the total current, at $E \geqslant E_{crit}$ and $t > 60$ s, can be written as

$$j = j_{dl} + j_{ox} + j_p \tag{7}$$

where j_{dl} can be neglected and j_{ox} is described by Equation 4.

The rising segments of the current-time transients obtained at pH 4.0 (Fig. 1(d)) show that the curves are dependent on the applied potential. A relationship between current and the square root of the time was found for 60 s $< t <$ 120 s (Fig. 5). After 120 s, an effective decrease in the nucleation rate (Fig. 6) is shown by the transition from an $i/t^{1/2}$ relationship to an $i/t^{3/2}$. Thus, the experimental current transients presented in Fig. 1(d) seems to be governed by a nucleation and growth process.

The data at pH 4.0 are in agreement with Hills' model [33], where $j_p = j_{ni} + j_{np}$, and can be represented by the equations:

$$j_{ni} = 2^{3/2} P_3 t^{1/2} \tag{8}$$

$$j_{np} = 4/3\, k_n P_3 t^{3/2} \tag{9}$$

where

$$P_3 = nFN_o\pi(D_o c)^{3/2} M^{1/2} \rho^{-1/2} \tag{10}$$

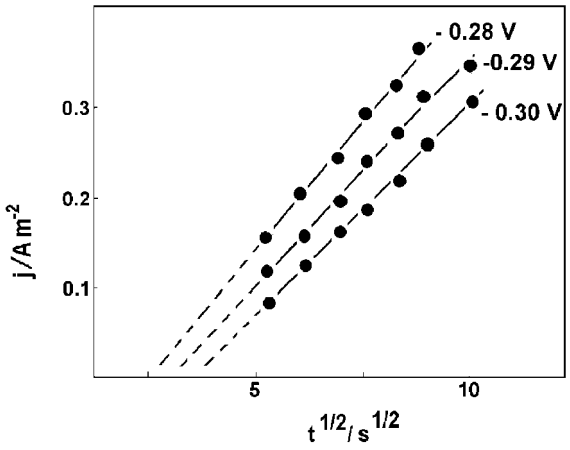

Fig. 4. Current density dependence on $t^{1/2}$ at constant potential, in 0.5 M $NaClO_4$, pH 4.0.

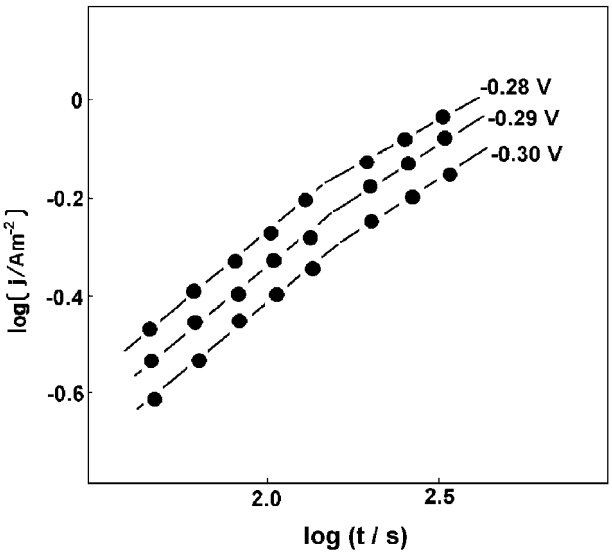

Fig. 5. Logarithmic plot of current density as function of time in 0.5 M $NaClO_4$, pH 4.0.

In the equations above, j_{ni} and j_{np} correspond to instantaneous and progressive nucleation currents, respectively, N_o represents the number of nuclei already present or instantaneously formed, D_o and c are the diffusion coefficient and the concentration of the dissolved material, k_n is the rate constant for nuclei formation, M and ρ the molecular weight and the density of the dissolved material and the other terms have their usual meaning.

The current density relationship with $t^{1/2}$ suggests that the pit growth process is an instantaneous three-dimensional nucleation followed by growth controlled by hemispherical diffusion [33]. The interception on the time axis at zero current indicates that an induction period (τ) is necessary to initiate the nucleation and growth processes (Fig. 4). The slope $dj_{ni}/dt^{1/2}$ allows the calculation of P_3 and substitution of P_3 into Equation 9 allows k_n to be evaluated (Table 2).

The rate constant for nuclei formation depends on the metal and on the applied perturbation characteristics. The marked dependence of the growth current on potential indicates that there is a distribution of the nucleation sites of different energies which nucleate at distinct potentials [33]. The increase of the rate constant, k_n, suggests that the more positive the applied potential the greater will be the number of the activated sites (Table 2). After 120 s, the decrease in the nucleation rate (Fig. 5), may be explained by the overlapping of the diffusion zones around each nucleus and, therefore, a progressive regime is detected at this stage of the transients.

The overall anodic current density of the system may be described as a sum of the components j_{dl}, j_{ox} and j_p (Equation 7). When $t < 60$ s, the variation $j_{ox}(t)$ is given by Equation 4 and $j_p = 0$. When 60 s $< t <$ 120 s, j_p equals j_{ni} (Equation 8) and in the case of $t >$ 120 s j_p may be represented by j_{np} (Equation 9).

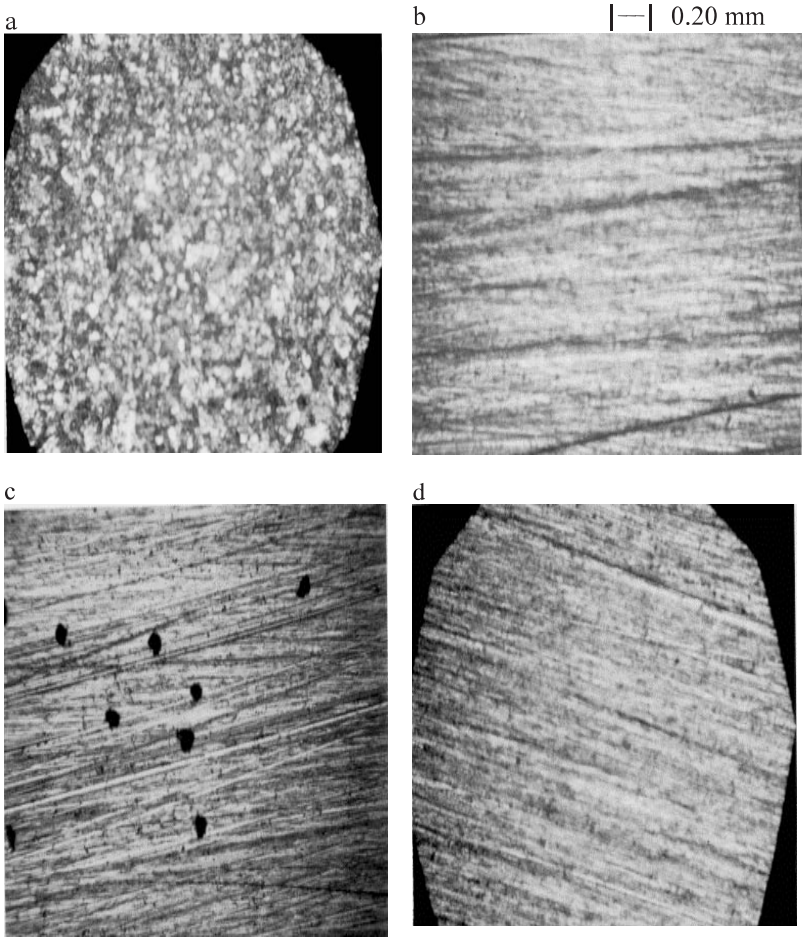

Fig. 6. Electrode surface after 5 min of potential holding at E_{crit}. (a) pH 2.0, in $NaClO_4$ 0.5 M, E_{crit} = –0.37 V; (b) pH 2.0, in $NaClO_4$ 0.5 M + 10^{-2} M of citric acid, E_{crit} = −0.26 V; (c) pH 3.0, in $NaClO_4$ 0.5 M, E_{crit} = −0.32 V; and (d) pH 3.0, in $NaClO_4$ 0.5 M + 10^{-2} M of citric acid, E_{crit} = −0.24 V.

The results for pit growth at pH 3.0 showed a current density dependence on t, instead of $t^{1/2}$ that did not allow comparison with the data obtained at pH 4.0.

3.2. *Tin/perchlorate, citric acid system*

The type of corrosion varies with pH in 0.5 M $NaClO_4$. At pH 1.0 and 2.0 the resulting surface, after 5 min of potential holding at E_{crit}, shows general corrosion (Fig. 6(a)) described as pitting initiation [26, 27]. At pH 3.0 and 4.0 the current increase occurs at more positive potentials (Fig. 6(c)) and pitting corrosion occurs. It is interesting to note that the difference between the type of corrosion found at pH 1.0 and 2.0 (general) and at pH 3.0 and 4.0 (pitting) may be associated not only with the solution acidity, but also with the presence of a film on the electrode surface [22]. This assumption is supported by the potentiodynamic profile of the metal at pH 3.0 and 4.0 where an anodic current peak, at about −0.35 V, indicates the formation of an oxide layer before breakdown potential (Fig. 2).

Table 2. P_3 parameters and rate constant for nuclei formation as function of applied potential, pH 4.0

E/V	$10^4 \times P_3$/A s$^{-1/2}$ m^{-2}	k_n/s^{-1}
−0.28	1.19	1.31
−0.29	1.03	1.23
−0.30	0.95	1.17

Figure 6(a) and (b) compare the surface of the electrode subjected for 5 min to the critical potential, at pH 2.0. The E_{crit} displacement, after reaching a citrate concentration of 10^{-2} M approaches 0.11 V and general corrosion is observed. After each citrate addition, the electrode surface shows an increase in number and size of areas where dissolution is more uniform. The characteristic corrosion promoted by the citric acid was identified in these areas where anisotropic reflection of polarized light was observed. The minimum concentration of the organic acid needed to inhibit pit nucleation is 10^{-2} M (Fig. 6(b)). At pH 3.0, the surface shows pitting corrosion (Fig. 6(c)). After each addition of citric acid, a decrease in the number of pits was noted. The minimum concentration of the organic acid to completely inhibit pitting of tin is 10^{-2} M (Fig. 6(d)) and the E_{crit} shift approaches 0.08 V.

The effect of the systematic additions of citric acid on the critical potential of tin in sodium perchlorate solution is shown in Fig. 7. In the pH range from 1.0 to 4.0, citrate additions shift E_{crit} to more positive

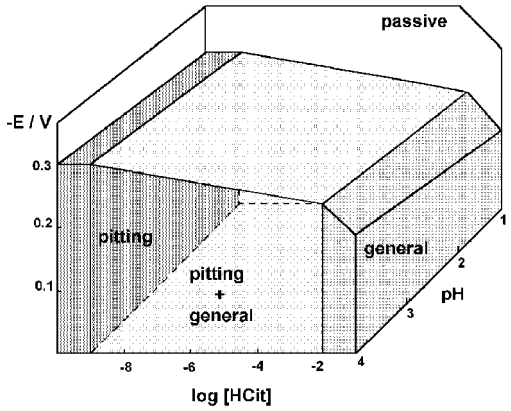

Fig. 7. Stability diagram of tin in solutions containing perchlorate and citrate anions, pH range from 1.0 to 4.0.

values. There is a linear dependence of E_{crit} on pH. At potentials more negative than the critical potential the electrode displays passive behaviour in the absence of citric acid. For solutions containing 10^{-2} M of citric acid the electrode surface exhibits no pitting corrosion. In the region between the two former regions, the inhibiting effect of the organic acid is incomplete and the electrode shows a mix of pitting and general corrosion.

Figure 7 shows also the E_{crit}–log[HCit] dependence at constant pH. When the citric acid concentration is in the range 10^{-9} M < [Hcit] < 10^{-2} M, there is a linear decay of E_{crit}. However, after reaching a citric acid concentration of 10^{-2} M a deflection is observed indicating that, from this point, the behaviour of the system changes. The diagram makes clear that, above an organic acid concentration of 10^{-2} M, general corrosion occurs and below this limit pitting corrosion is observed. The citrate anion effect is clearly identified by the increase in the E_{crit} value.

The current transients recorded in the presence of citric acid show that the induction period is longer than that observed in pure perchlorate (Table 3). Therefore, it can be suggested that the metal/citrate anion interactions are stronger than those of metal/perchlorate and/or the aggressive behaviour of ClO_4^- presence is weakened, favouring the formation of a more stable layer.

4. Conclusion

The critical potential was determined in 0.5 M sodium perchlorate in the pH range from 1.0 to 4.0. The results showed that the type of corrosion, pitting or general, depends on pH. At pH 3.0 and 4.0 the pit initiation is preceded by the formation of an oxide layer, described by a dissolution–precipitation model for metal passivation. Pit nucleation and growth involve a number of contributions which were distinguished through the analysis of current transients at constant potential. At pH 4.0, pit growth occurs in two steps and can, in principle, be described by instantaneous nucleation followed by progressive nucleation.

In general, compounds which inhibit pitting can promote general corrosion. The inhibiting effect of citric acid on pitting corrosion is recognised by the shift of the critical potentials to more positive values. Actually, the type of corrosion is closely related with the quantity of citrate anions. The minimum concentration of the organic acid to inhibit pitting of tin is 10^{-2} M.

Table 3. Induction period as function of citric acid concentration

[citrate]/M	pH *1.0* τ/s	pH *2.0* τ/s	pH *3.0* τ/s	pH *4.0* τ/s
0	3.0 ± 0.2	3.0 ± 0.2	5.0 ± 0.2	6.0 ± 0.2
10^{-7}	3.0 ± 0.2	4.0 ± 0.2	5.0 ± 0.2	6.0 ± 0.2
10^{-5}	4.0 ± 0.2	5.0 ± 0.2	6.0 ± 0.2	8.0 ± 0.2

Acknowledgement

The authors acknowledge useful discussions with Mrs Silvia H. Bonilla. Financial support from Fundação de Amparo à Pesquisa do Estado de São Paulo, FAPESP (procs. 82/746-2, *eq* 86/2143-4, 89/3488-2, 93/3353-8) and Conselho Nacional de Desenvolvimento Científico e Tecnológico, CNPq (procs. 13.3356/92, 301426/79, 840424/89) is gratefully recognized.

Reference

[1] T. P. Hoar, *Trans. Faraday Soc.* **30** (1934) 472.
[2] F. M. Jeffrey, *Trans. Faraday Soc.* **20** (1924) 390.
[3] E. L. Koehler, *J. Electrochem. Soc.* **103** (1956) 486.
[4] G. G. Kamm and A. R. Willey, *Corros. Sci.* **17** (1961) 99.
[5] J. J. Lingane, *J. Am. Chem. Soc.* **65** (1946) 866.
[6] R. P. G. Elbourne and G. S. Buchanan, *J. Inorg. Nucl. Chem.* **32** (1970) 493.
[7] R. P. G. Elbourne and G. S. Buchanan, *ibid.* **32** (1970) 3559.
[8] J. C. Sherlock and S. C. Britton, *Br. Corros. J.* **7** (1972) 180.
[9] J. C. Sherlock, J. H. Hancox and S. C. Britton, *ibid.* **7** (1972) 222.
[10] J.C. Sherlock, *ibid.* **10** (1975) 144.
[11] V. K. Gouda, E. N. Riskalla, S. Abd El Wahab and E. M. Ibrahim, *Corros. Sci.* **21** (1981) 1
[12] H. Leidheiser Jr, A. F. Hauch, E. M. Ibrahim and R. D. Granata, *J. Electrochem. Soc.* **129** (1982) 1651.
[13] J. C. Sherlock and S. C. Britton, *Br. Corros. J.* **8** (1973) 210
[14] P. G. Antonov and I. A. Agapov, *Zh. Prikl. Khim.* **61** (1988) 1723.
[15] J. M. Bastidas, J. J. Damborenea, J. A. Gonzalez, E. Otero, M. E. Chacon, W. I. Archer, J. D. Scantelbury and K. Alston, *Corros. Sci.* **30** (1990) 171.
[16] Y. M. Chen, T. J. O'Keefe and W. J. James, *Thin Solid Films* **129** (1985) 205.
[17] B. F. Giannetti, P. T. A. Sumodjo and T. Rabockai, *J. Appl. Electrochem.* **20** (1990) 672.
[18] B. F. Giannetti, P. T. A. Sumodjo, T. Rabockai, A. M. Souza and J. Barbosa, *Electrochim. Acta* **37** (1992) 143.
[19] B. F. Giannetti and T. Rabockai, Anais Assoc. Brasil. Quím., **43** (1994) 1.
[20] M. Seruga and M. Metikos-Hukovic, *J. Electroanal. Chem.* **334** (1992) 223.
[21] S. A. M. Refaey and S. S. Abd El Rehim, *Electrochim. Acta* **42** (1996) 667.
[22] C. M. V. Almeida, B. F. Giannetti and T. Rabockai, *J. Electroanal. Chem.* **422** (1997) 185.
[23] N. D. Kim and A. M. Sukhotin, *Zh. Prikl. Khim.* **63** (1990) 1737.

[24] *Idem, ibid.* **63** (1990) 1818.
[25] S. Szklarska-Smialowska, 'Pitting Corrosion of Metals', NACE, Houston (1986).
[26] J. R. Galvele, *J. Electrochem. Soc.* **123** (1976) 464.
[27] E. A. Lizlous and A. P. Bond, *Corros. J.* **31** (1975) 219.
[28] R. Tunold and A. Broli, *Corros. Sci.* **13** (1973) 361.
[29] M. L. Rumpel, A. W. Davidson and J. Kleinberg, *Inorg. Chem.* **3** (1964) 935.
[30] M. E. Straumanis and M. Duta, *Inorg. Chem.* **5** (1966) 992
[31] M. Bojinov, K. Salmi and G. Sundholm, *J. Electroanal. Chem.* **347** (1993) 207.
[32] K. Ogura, *Electrochim. Acta* **25** (1980) 335.
[33] G. J. Hills, D. J. Schiffrin and J. Thompson, *Electrochim. Acta.* **19** (1974) 657.